

Emulsion Designer Using Microfluidic Three-Dimensional Droplet Printing in Droplet

Li Chen, Yao Xiao, Qinglin Wu, Xiaoxiao Yan, Peng Zhao, Jian Ruan, Jianzhen Shan, Dong Chen,* David A. Weitz, and Fangfu Ye*

Hierarchical emulsions are interesting for both scientific researches and practical applications. Hierarchical emulsions prepared by microfluidics require complicated device geometry and delicate control of flow rates. Here, a versatile method is developed to design hierarchical emulsions using microfluidic 3D droplet printing in droplet. The process of droplet printing in droplet mimics the dragonfly laying eggs and has advantages of easy processing and flexible design. To demonstrate the capability of the method, double emulsions and triple emulsions with tunable core number, core size, and core composition are prepared. The hierarchical emulsions are excellent templates for the developments of functional materials. Flattened crescent-moon-shaped particles are then fabricated using double emulsions printed in confined 2D space as templates. The particles are excellent delivery vehicles for 2D interfaces, which can load and transport cargos through a well-defined trajectory under external magnetic steering. Microfluidic 3D droplet printing in droplet provides a powerful platform with improved simplicity and flexibility for the design of hierarchical emulsions and functional materials.

disadvantages of low efficiency and poor controllability over the emulsion size, core size, core number and core composition.^[1,2] With the advent of microfluidic technology, which could precisely control the emulsification process, complex hierarchical emulsions with tunable emulsion size, core size, and core number have been prepared using PDMS or glass capillary microfluidic devices.^[3–7] The hierarchical emulsions have demonstrated a wide range of applications in chemical reaction,^[8,9] drug delivery,^[10–14] cell culture,^[15–19] organ on a chip,^[20–22] functional material,^[23–29] and so on. Despite the advances, the preparation of hierarchical emulsions by microfluidics generally requires complicated device geometry and delicate control of flow rates. Therefore, innovations of novel techniques with improved simplicity and flexibility are needed.

1. Introduction

Hierarchical emulsions with tunable structure and composition are of great interest for chemistry, chemical engineering, material science, and medicine. Conventional emulsification methods, which lacks the control of the emulsification process, could only prepare some simple emulsions, such as water-in-oil-in-water or oil-in-water-in-oil double emulsions, by successively emulsifying one phase in the other phase and have

To meet the demands, the combination of microfluidics and 3D printing is emerging as a powerful tool, which provides a simple and flexible control over the emulsification process.^[30–35] For example, continuous extrusion of liquid metal in carbopol hydrogel via a 3D printing system allows the design and construction of 3D structures and electronic systems;^[36] elastomers with tunable compositions and properties are prepared using the combined technique;^[37] biomimetic systems with synergetic color and shape responses are developed using microfluidic 3D

Dr. L. Chen, Y. Xiao, Q. Wu, X. Yan, Prof. P. Zhao,
Prof. J. Ruan, Prof. J. Shan, Prof. D. Chen
Department of Medical Oncology
The First Affiliated Hospital
School of Medicine
Zhejiang University
Hangzhou, Zhejiang 310003, P. R. China
E-mail: chen_dong@zju.edu.cn

Dr. L. Chen, Prof. F. Ye
Wenzhou Institute
University of Chinese Academy of Sciences
Wenzhou, Zhejiang 325001, P. R. China
E-mail: fye@iphy.ac.cn

Prof. D. Chen
College of Energy Engineering and State Key Laboratory
of Fluid Power and Mechatronic Systems
Zhejiang University
Hangzhou, Zhejiang 310027, P. R. China

Prof. D. A. Weitz
John A. Paulson School of Engineering and Applied Sciences
Harvard University
Cambridge, MA 02138, USA

Prof. F. Ye
Beijing National Laboratory for Condensed Matter Physics
Institute of Physics
Chinese Academy of Sciences
Beijing 100190, P. R. China

 The ORCID identification number(s) for the author(s) of this article can be found under <https://doi.org/10.1002/smll.202102579>.

DOI: 10.1002/smll.202102579

printing.^[38] The progresses have demonstrated that microfluidic 3D printing is suitable to serve as a platform for the design and development of functional materials.^[39] However, the preparations of complex hierarchical emulsions using microfluidic 3D droplet printing in droplet haven't been studied yet and the developments of related functional materials haven't been explored.

In this paper, we develop a facile method for the preparation of hierarchical emulsions by microfluidic 3D droplet printing in droplet. The combination of microfluidics and 3D printing allows the precise control of droplet printing in droplet and is advantageous in designing hierarchical emulsions. Detailed investigations of the printing process reveal that the detachment of droplets from the nozzle strongly depends on middle oil viscosity, middle oil density, inner droplet size, and nozzle diameter. Double and triple emulsions with tunable core number, core size, and core composition are demonstrated. Flattened crescent-moon-shaped particles are then developed using double emulsions confined in 2D space as templates. The particles are excellent delivery vehicles for 2D interfaces, which are able to load and transport cargos through a well-defined trajectory under external magnetic steering, showing great potentials for applications.

2. Results and Discussion

Carbopol hydrogel, a transparent shear-thinning material, is chosen as the supporting matrix for droplet printing.^[39–41]

The optimized concentration of the hydrogel matrix in water is determined to be 0.1 wt%, at which droplets could be stabilized at a fixed position in 3D space and reconfigure to spherical shape after printing. To print droplets, a microfluidic 3D droplet printing system is developed by modifying an extrusion-based 3D printer, in which a tapered glass capillary is mounted on the printer head and connected with a syringe pump by a polyethylene tube. The 3D printing system is used to precisely control the position of the printer head and the infusion of the syringe pump via programmable codes. Arrays of discrete oil droplets are first printed in the hydrogel matrix by extruding a fixed amount of oil at predesigned positions, which will detach from the glass capillary nozzle under the viscous drag of the hydrogel matrix as the nozzle rises. Since oil droplets are stabilized in the hydrogel matrix, water cores could subsequently be printed in the oil droplets by virtue of the precise control, achieving water-in-oil-in-water double emulsions, as shown in **Figure 1a**. The droplet printing process is similar to interfacial emulsification,^[16,42,43] which mimics female dragonfly laying eggs in water using the tip of its abdomen.^[44] When water is extruded out of the nozzle, which is then lifted up, the detachments of the inner fluid tip from the nozzle are mainly determined by surface tension, which holds the inner fluid tip to the nozzle, and viscous force, which drags the inner fluid tip off the nozzle. In surface tension-dominated regime, the inner fluid tip moves up with the nozzle and is pinched off the nozzle at the oil/hydrogel interface, which repels the water/oil interface, as shown in **Figure 1b** and **Movie S1**, Supporting Information. In viscous force-dominated regime, the viscous drag is strong

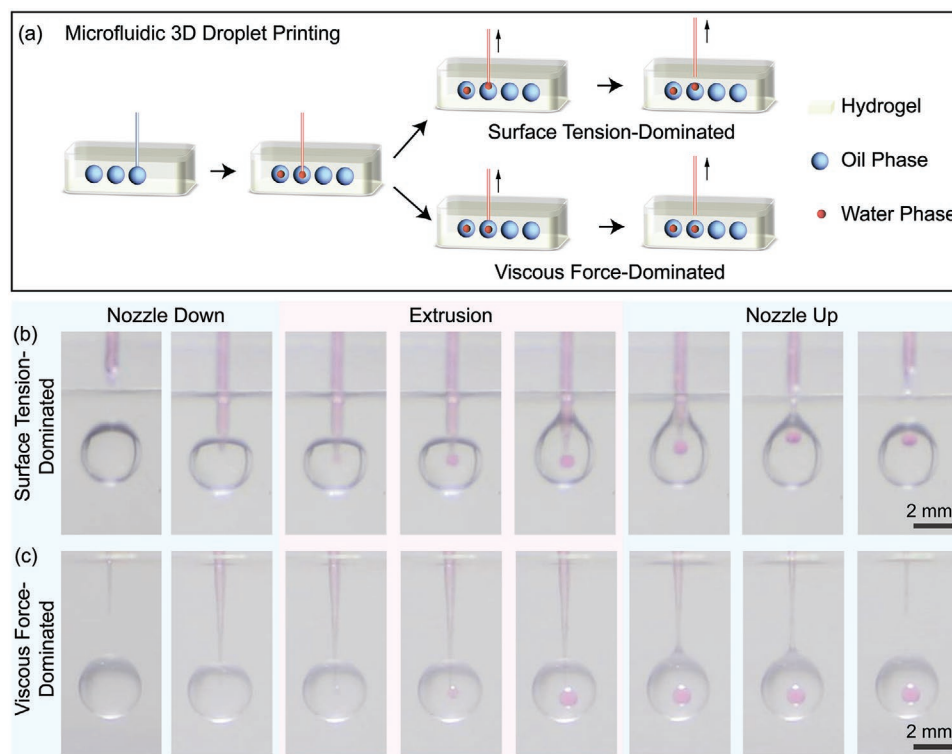


Figure 1. Microfluidic 3D droplet printing in droplet. a) Schematics showing surface tension-dominated and viscous force-dominated droplet printing in droplet. Sequences of snapshots showing the processes of b) surface tension-dominated and c) viscous force-dominated droplet printing in droplet. The inner core is water with 2 wt% PVA and the shell is silicone oil with 2 wt% $\text{NH}_2\text{-PDMS-NH}_2$.

enough to overcome the surface tension, thus pulling the inner fluid tip off the nozzle when the nozzle is ascending, as shown in Figure 1c and Movie S2, Supporting Information.

To systematically investigate the behaviors of droplet printing in droplet and reveal the underlying mechanisms of droplet formation, we use silicone oils with different viscosity and density as the model middle oil phase and carefully analyze the forces exerted on the inner fluid tip when elevating the nozzle. When the nozzle is ascending slowly at a constant speed, it is reasonable to assume that the forces exerted on the inner fluid tip are at equilibrium, having $F_s = F_v + G - F_b$, where F_s is the surface tension, F_v is the viscous force, G is the gravity, and F_b is the buoyancy. Among the forces, the surface tension $F_s = \pi\phi\gamma_{o/w}$ tends to hold the inner fluid tip to the nozzle, where ϕ is the nozzle diameter and $\gamma_{o/w}$ is the surface tension between oil and water; the viscous force $F_v = 3\pi\eta\nu D$ tends to drag the inner fluid tip off the nozzle, where η is the viscosity of the oil phase, ν is the moving speed of the nozzle, and D is the droplet diameter; the gravity $G = \rho_w gV$ tends to pull the inner fluid tip downwards, where ρ_w is the density of the water phase, g is the acceleration of gravity, and V is the volume of the inner fluid tip; the buoyancy $F_b = \rho_o gV$ tends to lift the inner fluid tip upwards, where ρ_o is the density of the oil phase. To quantitatively compare the forces, Bond number $Bo = (gravity - buoyancy)/surface\ tension = (G - F_b)/F_s$ and capillary number $Ca = viscous\ force/surface\ tension = F_v/F_s$ of oils with different viscosities and densities are calculated, as shown in detail in Table 1, Supporting Information. In most cases, the Bond number is on the scale of $Bo = 10^{-3} - 10^{-1}$, which suggests that the gravity and buoyancy of the inner fluid tip are generally cancelled out with each other due to the small density difference between oil and water and could be ignored when compared to the surface tension. The capillary number is calculated to be $Ca = 10^{-4} - 10^0$, implying that in most cases the viscous force is smaller than the surface tension and could not drag the inner fluid tip off the nozzle when the nozzle is ascending. When the oil phase has a large viscosity, for example, PDMS with $\eta = 5000\text{ mPa}\cdot\text{s}$, the capillary number is on the order of $\approx 10^0 - 10^2$, and the inner fluid tip could be dragged off the nozzle by the viscous force.

In addition to viscosity and density, droplet size and nozzle diameter also play an important role in the process of droplet formation. Phase diagram of microfluidic 3D droplet printing in droplet as a function of inner droplet diameter D (ranging from 0.75 to 3 mm) and nozzle diameter ϕ (ranging from 50 to 1000 μm) is systematically shown in Figure 2. When the droplet diameter is large and the nozzle diameter is small (blue region marked by triangles), viscous force dominates and is strong enough to drag the inner fluid tip off the nozzle as the nozzle arises. When the droplet diameter decreases or the nozzle diameter increases (red region marked by circles), the surface tension starts to dominate; the inner fluid tip could only detach from the nozzle when the inner fluid tip reaches the oil/hydrogel interface, whose surface tension F_i ($\gamma_{o/c} \approx 35\text{ mN m}^{-1}$) is strong enough to overcome the oil/water surface tension F_s ($\gamma_{o/w} \approx 20\text{ mN m}^{-1}$) and repel the inner fluid tip off the nozzle. Interestingly, the boundary that separates viscous force-dominated regime and surface tension-dominated regime manifests a linear relationship between D and ϕ , which is consistent with theoretical prediction that $Ca = F_v/F_s \approx D/\phi$. When the droplet

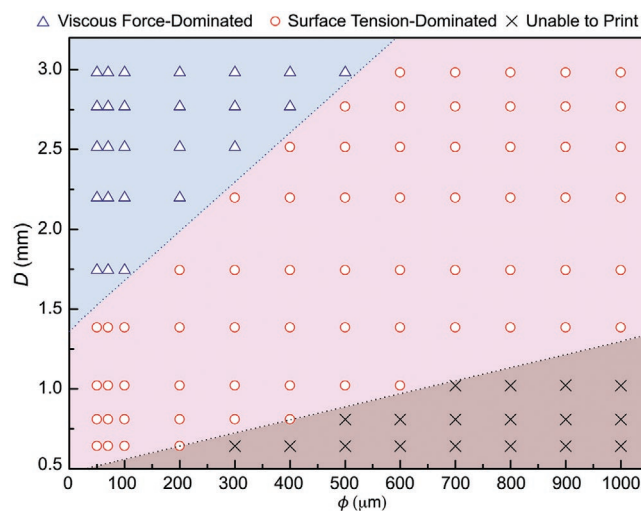


Figure 2. Phase diagram of microfluidic 3D droplet printing in droplet as a function of droplet diameter, D , and nozzle diameter, ϕ . Triangles, circles, and crosses represent viscous force-dominated regime, surface tension-dominated regime, and unable to print, respectively. The viscosity of the middle oil phase is kept constant at $\eta = 200\text{ mPa}\cdot\text{s}$ and the elevating speed of the nozzle is fixed at $\nu = 2\text{ mm s}^{-1}$.

diameter is comparable to or smaller than the nozzle diameter (grey region marked by crosses), the repulsion of the oil/water interface is not able to pull the inner fluid tip off the nozzle, resulting in failure of droplet printing in droplet. Therefore, to print small droplets, small nozzle diameter is preferred.

Microfluidic 3D droplet printing in droplet provides a versatile platform for the design of hierarchical emulsions with tunable core number, core size, and core composition. The platform could directly print inner cores in existing droplets, simply by lowering the nozzle down into the droplets, extruding the inner phase, and then lifting the nozzle up. Water-in-oil-in-water double emulsions with core number varying from one to seven are thus prepared by printing water cores in the same oil droplet, as shown in Figure 3a and Figure S1a and Movie S3, Supporting Information. In addition, the size of water core can simply be adjusted by controlling the extruded volume through programming, as shown in Figure 3b and Figure S1b and Movie S4, Supporting Information. By virtue of the precise control, double emulsions with controlled core composition, containing tunable numbers of water cores and glycerol cores, could also be fabricated, as shown in Figure 3c–e and Figure S2, Supporting Information.

High-order hierarchical emulsions could be prepared following the same strategy, that is, successively printing droplets in droplet. For example, oil-in-water-in-oil-in-water triple emulsions with tunable inner core number, middle core number and inner core composition are prepared by sequential droplet printing in droplet, as shown in Figure 4a–f and Figure S3 and Movie S5, Supporting Information. The triple emulsions are prepared by first printing the oil droplets in hydrogel, next printing the middle water cores in the oil droplets, and last printing the inner oil cores in the middle water cores.

Microfluidic 3D droplet printing in droplet is advantageous in constructing hierarchical emulsions and has several advantages when compared with microfluidics: i) Microfluidics highly

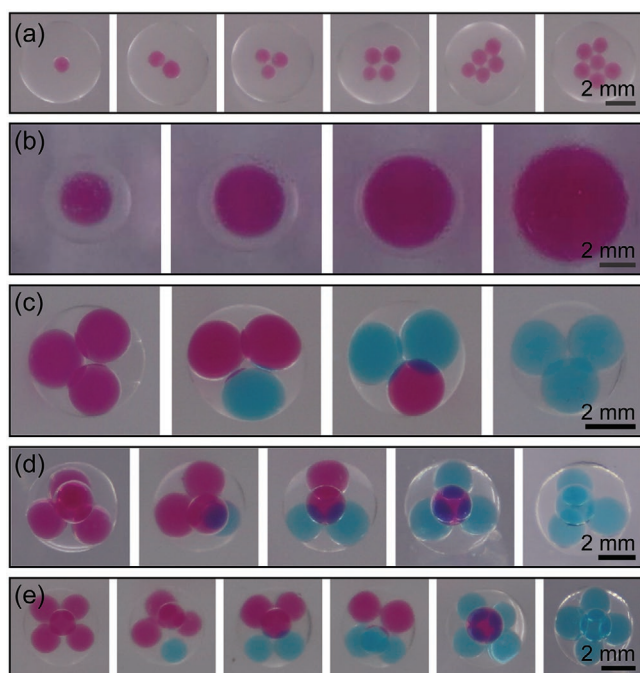


Figure 3. Flexible preparation of water-in-oil-in-water double emulsions using microfluidic 3D droplet printing in droplet. Double emulsions with tunable a) core number, b) core size, and c–e) core composition. The red inner cores are water with 2 wt% PVA dyed by a red ink. The blue inner cores are glycerol with 2 wt% PVA dyed by a blue ink. The shell is silicon oil with 2 wt% $\text{NH}_2\text{-PDMS-NH}_2$. If unspecified, the silicon oil has a viscosity of $\eta = 200$ mPa·s.

relies on device geometry to achieve hierarchical emulsions, for example, the combination of co-flowing and flow-focusing geometries for double emulsions. Microfluidic 3D droplet printing could directly print inner cores in existing droplets. ii) When using microfluidic devices, it generally requires delicate adjustments of the flow rates of the inner, middle, and outer phases to control the core size and core number. The core size and core number could simply be controlled by adjusting the amount of extruded phase and the times of printing when using droplet printing. iii) It is generally hard to achieve hierarchical emulsions with controlled core composition using microfluidics. The droplet printing platform is able to fabricate double and triple emulsions with controlled core compositions, for example, the double emulsions with glycerol cores sinking at the droplet bottom and water cores floating at the droplet top, as shown in Figure S4, Supporting Information.

Hierarchical emulsions are excellent templates for the design of functional materials. To prepare solid particles, polymerizable oils, for example, PDMS, are used as the middle oil phase and solid particles with tunable shell thickness, core size, and core number are prepared using water-in-oil-in-water double emulsions as templates, as shown in Figures S5 and S6, Supporting Information. The solid PDMS particles could further be functionalized by printing magnetic fluids in the cores, as shown in Figure S7, Supporting Information, and the magnetic particles could be steered through a well-defined trajectory under an external magnetic field, as shown in Figure S8 and Movie S6, Supporting Information.

To demonstrate the applications of the hierarchical particles, we use flattened water-in-oil-in-water double emulsions

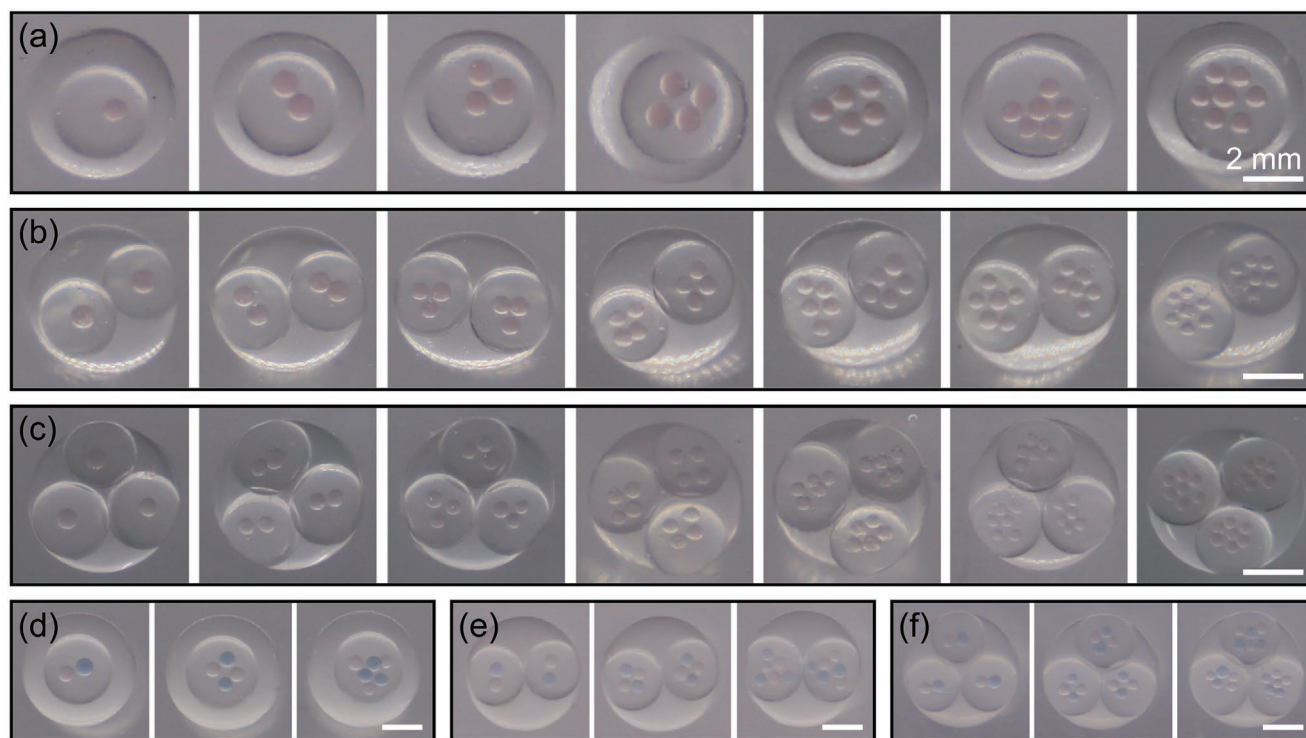


Figure 4. Flexible preparation of oil-in-water-in-oil-in-water triple emulsions by sequential droplet printing in droplet. Triple emulsions with tunable a) inner core number, b,c) middle core number, and d–f) inner core composition.

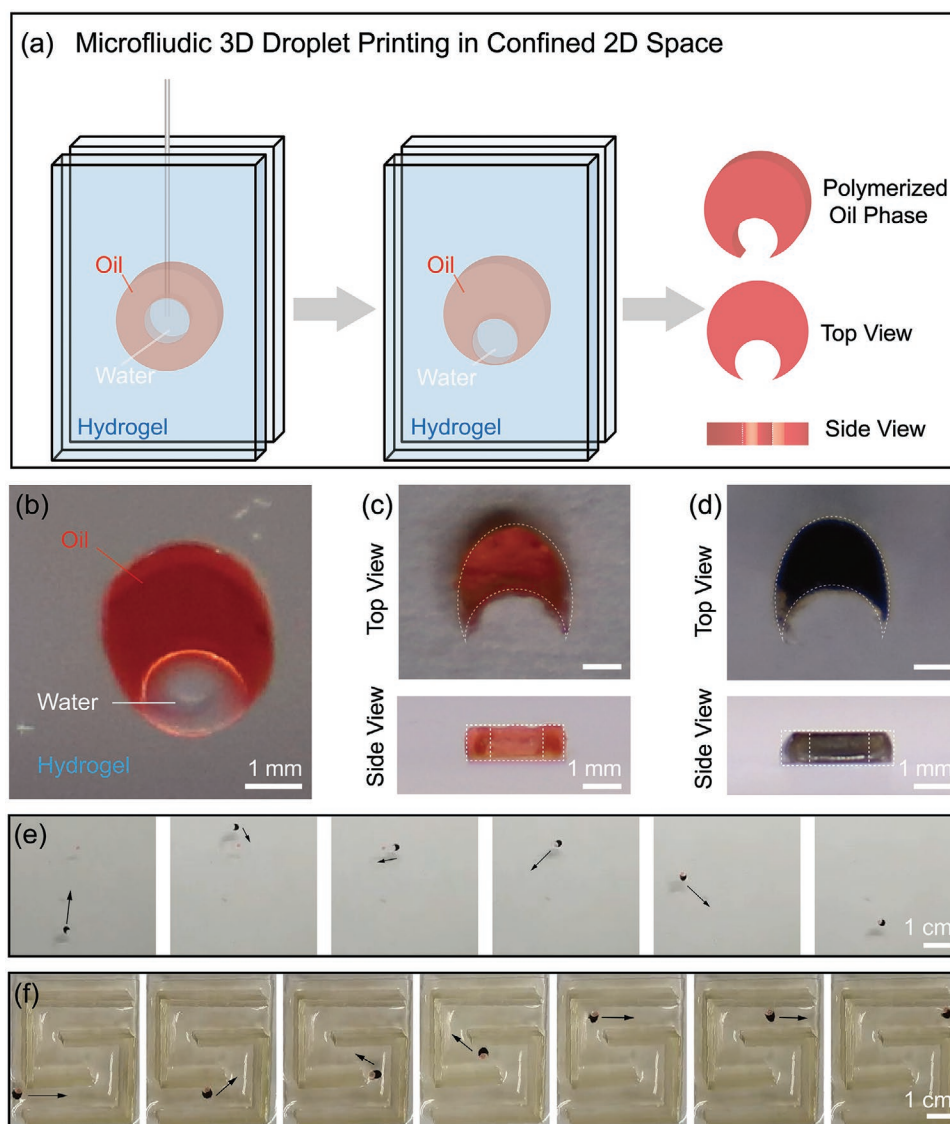


Figure 5. Microfluidic 3D droplet printing in confined 2D space. a) Preparation of flattened crescent-moon-shaped particles using droplet printing in droplet in confined 2D space. b) Optical image of a water-in-oil-in-water double emulsion confined between two parallel glass plates. Optical image of c) a PDMS particle and d) a magnetic PDMS particle with a flattened crescent-moon shape after thermal polymerization and removal of the water core. e) Loading and transporting a cargo using a flattened crescent-moon-shaped particle at the water/air interface under the steering of an external magnetic field. f) Transporting a cargo at the water/air interface through a maze with a well-defined trajectory.

confined between two parallel plates as templates, which is prepared by droplet printing in confined 2D space, and fabricate flattened crescent-moon-shaped particles, as schematically shown in **Figure 5a**. Because the spacing of the two plates is smaller than the core, the double emulsion is flattened into a 2D disk, as shown in **Figure 5b**. After polymerization of the middle oil phase and removal of the inner water phase, flattened crescent-moon-shaped PDMS particles with and without magnetic nanoparticles are achieved, as shown in **Figures 5c,d**, respectively. The flattened crescent-moon-shaped magnetic particles are ideal delivery vehicles for 2D interfaces. The particle at the air/water interface tends to load the cargo stably in its concave, which is attributed to the deformation of the air/water interface created by the particle, as shown in **Figure 5e**

and **Movie S7**, Supporting Information. After loading, the particle is able to precisely transport the cargo through a maze with a well-defined trajectory under the steering of an external magnetic field at the air/water interface, as shown in **Figure 5f** and **Movie S8**, Supporting Information, or at the oil/water interface, as shown in **Figure S9** and **Movie S9**, Supporting Information.

Microfluidic 3D droplet printing in droplet, which represents a versatile platform for the design of hierarchical emulsions, has advantages of easy processing and flexible design, and is capable of constructing hierarchical emulsions with tunable core number, core size, and core composition. However, because hierarchical emulsions are prepared by sequential droplet printing, the emulsion size is mainly limited by

the resolution of the x - y - z movements of the 3D printer and the nozzle diameter. When the resolution of the x - y - z movements of the 3D printer is 100 μm and the nozzle diameter is 50 μm , the droplet printing system is able to prepare hierarchical emulsions with diameter, d , ranging from ≈ 500 to ≈ 3000 μm , as shown in Figure S10, Supporting Information. In addition, successive preparation of double emulsions using microfluidic 3D droplet printing is estimated to be 300 double emulsions per hour when the emulsion diameter, d , is ≈ 2 mm, as shown in Movie S10, Supporting Information. One possible solution to scale up is to use multiple nozzles for parallel printing.

3. Conclusion

Here, we develop a versatile method to design hierarchical emulsions using microfluidic 3D droplet printing in droplet. The printing of droplet in droplet mimics the dragonfly laying eggs, and the detachment of droplets from the nozzle is either dominated by surface tension or viscous force. Compared with microfluidics, microfluidic 3D droplet printing in droplet has advantages of easy processing and flexible design, and is capable of constructing hierarchical emulsions with tunable core number, core size, and core composition. Flattened crescent-moon-shaped particles are then fabricated using double emulsions confined in 2D space as templates. When served as delivery vehicles, the particles demonstrate excellent performances in loading and transporting cargos under the steering of an external magnetic field. The combination of microfluidics and 3D printing has demonstrated a powerful tool for scientific researches. It shows great potential at material designing and engineering, especially at the aspect of endowing droplets with tunable compositions and versatile functionalities, devoted to areas such as soft robotics, soft sensors, and biomedical assays.

Supporting Information

Supporting Information is available from the Wiley Online Library or from the author.

Acknowledgements

This work was supported by the National Key Research and Development Program of China (2020YFA0908200), National Natural Science Foundation of China (Grant No. 21878258), Zhejiang Provincial Natural Science Foundation of China (Grant No. Y20B060027), and Zhejiang University Education Foundation Global Partnership Fund and Innovation Project of Keqiao. This work was also supported by the National Science Foundation (DMR1310266) and the Harvard Materials Research Science and Engineering Center (DMR-1420570).

Conflict of Interest

The authors declare no conflict of interest.

Data Availability Statement

Research data are not shared.

Keywords

droplets, emulsions, microfluidics, particles, three-dimensional printing

Received: April 30, 2021

Revised: June 8, 2021

Published online: August 12, 2021

- [1] A. Håkansson, *Annu. Rev. Food Sci. Technol.* **2019**, *10*, 239.
- [2] X. Huang, R. Fang, D. Wang, J. Wang, H. Xu, Y. Wang, X. Zhang, *Small* **2015**, *11*, 1537.
- [3] S.-H. Kim, D. A. Weitz, *Angew. Chem., Int. Ed.* **2011**, *50*, 8731.
- [4] C.-H. Choi, D. A. Weitz, C.-S. Lee, *Adv. Mater.* **2013**, *25*, 2536.
- [5] L.-Y. Chu, A. S. Utada, R. K. Shah, J. Kim, D. A. Weitz, *Angew. Chem., Int. Ed.* **2007**, *46*, 8970.
- [6] R. K. Shah, H. C. Shum, A. C. Rowat, D. Lee, J. J. Agresti, A. S. Utada, L.-Y. Chu, J.-W. Kim, A. Fernandez-Nieves, C. J. Martinez, D. A. Weitz, *Mater. Today* **2008**, *11*, 18.
- [7] A. R. Abate, J. Thiele, D. A. Weitz, *Lab Chip* **2011**, *11*, 253.
- [8] H. Song, D. L. Chen, R. F. Ismagilov, *Angew. Chem., Int. Ed.* **2006**, *45*, 7336.
- [9] H. Wang, Z. Zhao, Y. Liu, C. Shao, F. Bian, Y. Zhao, *Sci. Adv.* **2018**, *4*, eaat2816.
- [10] Z. Sun, C. Yang, F. Wang, B. Wu, B. Shao, Z. Li, D. Chen, Z. Yang, K. Liu, *Angew. Chem., Int. Ed.* **2020**, *59*, 9365.
- [11] C.-X. Zhao, D. Chen, Y. Hui, D. A. Weitz, A. P. J. Middelberg, *ChemPhysChem* **2016**, *17*, 1553.
- [12] H. Zhang, W. Cui, X. Qu, H. Wu, L. Qu, X. Zhang, E. Mäkilä, J. Salonen, Y. Zhu, Z. Yang, D. Chen, H. A. Santos, M. Hai, D. A. Weitz, *Proc. Natl. Acad. Sci. USA* **2019**, *116*, 7744.
- [13] Z. Sun, B. Wu, Y. Ren, Z. Wang, C.-X. Zhao, M. Hai, D. A. Weitz, D. Chen, *ChemPlusChem* **2021**, *86*, 49.
- [14] F. Liu, Y. Niko, R. Bouchaala, L. Mercier, O. Lefebvre, B. Andreiuk, T. Vandamme, J. G. Goetz, N. Anton, A. Klymchenko, *Angew. Chem., Int. Ed.* **2021**, *133*, 6647.
- [15] Q. Sun, S. Tan, Q. Chen, R. Ran, Y. Hui, D. Chen, C.-X. Zhao, *ACS Biomater. Sci. Eng.* **2018**, *4*, 4425.
- [16] S. Liao, Y. Tao, W. Du, Y. Wang, *Langmuir* **2018**, *34*, 11655.
- [17] P. Xu, X. Zheng, Y. Tao, W. Du, *Anal. Chem.* **2016**, *88*, 3171.
- [18] B. Wang, A. Ghaderi, H. Zhou, J. Agresti, D. A. Weitz, G. R. Fink, G. Stephanopoulos, *Nat. Biotechnol.* **2014**, *32*, 473.
- [19] S. Täuber, E. von Lieres, A. Grünberger, *Small* **2020**, *16*, 1906670.
- [20] Q. Chen, S. Utech, D. Chen, R. Prodanovic, J.-M. Lin, D. A. Weitz, *Lab Chip* **2016**, *16*, 1346.
- [21] Y. K. Jo, D. Lee, *Small* **2020**, *16*, 1903736.
- [22] A. C. Daly, L. Riley, T. Segura, J. A. Burdick, *Nat. Rev. Mater.* **2020**, *5*, 20.
- [23] B. Wu, Z. Sun, J. Wu, J. Ruan, P. Zhao, K. Liu, C. Zhao, J. Sheng, T. Liang, D. Chen, *Angew. Chem., Int. Ed.* **2021**, *60*, 9284.
- [24] B. Wu, C. Yang, B. Li, L. Feng, M. Hai, C.-X. Zhao, D. Chen, K. Liu, D. A. Weitz, *Small* **2020**, *16*, 2002716.
- [25] X. Xie, W. Zhang, A. Abbaspourrad, J. Ahn, A. Bader, S. Bose, A. Vegas, J. Lin, J. Tao, T. Hang, H. Lee, N. Iverson, G. Bisker, L. Li, M. S. Strano, D. A. Weitz, D. G. Anderson, *Nano Lett.* **2017**, *17*, 2015.
- [26] Z. Sun, C. Yang, M. Eggersdorfer, J. Cui, Y. Li, M. Hai, D. Chen, D. A. Weitz, *Chin. Chem. Lett.* **2020**, *31*, 249.
- [27] C. Nam, J. Yoon, S. A. Ryu, C.-H. Choi, H. Lee, *ACS Appl. Mater. Interfaces* **2018**, *10*, 40366.

- [28] C. Mou, W. Wang, Z. Li, X. Ju, R. Xie, N. Deng, J. Wei, Z. Liu, L.-Y. Chu, *Adv. Sci.* **2018**, 5, 1700960.
- [29] L. Kong, X. Jin, D. Hu, L. Feng, D. Chen, H. Li, *Chin. Chem. Lett.* **2019**, 30, 2351.
- [30] J. Zhao, N. He, *J. Mater. Chem. B* **2020**, 8, 10474.
- [31] A. K. Grosskopf, R. L. Truby, H. Kim, A. Perazzo, J. A. Lewis, H. A. Stone, *ACS Appl. Mater. Interfaces* **2018**, 10, 23353.
- [32] J. Wang, H. Le-The, Z. Wang, H. Li, M. Jin, A. van den Berg, G. Zhou, L. I. Segerink, L. Shui, J. C. T. Eijkel, *ACS Nano* **2019**, 13, 3638.
- [33] H. Cui, Y. Yu, X. Li, Z. Sun, J. Ruan, Z. Wu, J. Qian, J. Yin, *J. Mater. Chem. B* **2019**, 7, 7207.
- [34] Y. Yao, C. Yin, S. Hong, H. Chen, Q. Shi, J. Wang, X. Lu, N. Zhou, *Chem. Mater.* **2020**, 32, 8868.
- [35] R. L. Truby, M. Wehner, A. K. Grosskopf, D. M. Vogt, S. G. M. Uzel, R. J. Wood, J. A. Lewis, *Adv. Mater.* **2018**, 30, 1706383.
- [36] Y. Yu, F. Liu, R. Zhang, J. Liu, *Adv. Mater. Technol.* **2017**, 2, 1700173.
- [37] H. J. Mea, L. Delgadillo, J. Wan, *Proc. Natl. Acad. Sci. USA* **2020**, 117, 14790.
- [38] C. Yang, B. Wu, J. Ruan, P. Zhao, L. Chen, D. Chen, F. Ye, *Adv. Mater.* **2021**, 33, 2006361.
- [39] A. Z. Nelson, B. Kundukad, W. K. Wong, S. A. Khan, P. S. Doyle, *Proc. Natl. Acad. Sci. USA* **2020**, 117, 5671.
- [40] D. Bonn, M. M. Denn, *Science* **2009**, 324, 1401.
- [41] L. Ning, R. Mehta, C. Cao, A. Theus, M. Tomov, N. Zhu, E. R. Weeks, H. Bauser-Heaton, V. Serpooshan, *ACS Appl. Mater. Interfaces* **2020**, 12, 44563.
- [42] S. Liao, Y. He, D. Wang, L. Dong, W. Du, Y. Wang, *Adv. Mater. Technol.* **2016**, 1, 1600021.
- [43] J. Yun, X. Zheng, P. Xu, X. Zheng, J. Xu, C. Cao, Y. Fu, B. Xu, X. Dai, Y. Wang, H. Liu, Q. Yi, Y. Zhu, J. Wang, L. Wang, Z. Dong, L. Huang, Y. Huang, W. Du, *Small* **2020**, 16, 1903739.
- [44] P. S. Corbet, *Dragonflies: Behaviour and Ecology of Odonata*, Harley Books, Colchester **1999**.